Proceedings of the ASME 2009 Dynamic Systems and Control Conference
DSCC2009
October 12-14, 2009, Hollywood, California, USA

DSCC2009-2784

OPTIMAL-CONTROL METHODS FOR DESIGN OF TWO-DEGREE-FREEDOM SYSTEMS FOR NANOPOSITIONING

C. Lee
Department of Mechanical Science and Engineering
University of Illinois at Urbana-Champaign
Urbana, IL 61801 Email: clee62@illinois.edu

S. Salapaka *
Department of Mechanical Science and Engineering
University of Illinois at Urbana-Champaign
Urbana, IL 61801 Email: salapaka@illinois.edu

ABSTRACT

This paper presents, reviews, compares, and analyzes optimal-control methods for designing two-degree-of-freedom (2DOF) control laws for nanopositioning. The different methods are motivated by various practical scenarios and difficulty in achieving simultaneously multiple performance objectives of resolution, bandwidth, and robustness by tuning-based or shaping-of-open-loop-plants based designs. In this context, we study fundamental trade-offs between these performance objectives in 2DOF control designs for nanopositioning systems. In particular, in terms of the trade-offs, our analysis shows that the primary role of feedback is providing robustness to the closed-loop device whereas the feedforward component is mainly effective in overcoming fundamental algebraic constraints that limit the feedback-only designs. Experimental results indicate substantial improvements (over 200% *in bandwidth) when compared to optimal feedback-only controllers.*

1 INTRODUCTION

The development of micro cantilever-based devices has played a key role in advances of nanotechnology over the last two decades. By using a microcantilever with a sharp tip as a sensor, these devices can sense extremely small physical signals, such as tip-sample tunneling current in scanning tunneling microscope (STM) [1] and interatomic forces in atomic force microscope (AFM) [2]. Their capability of manipulation at atomic scale, together with the capability of sensing a variety of physical signals in diverse environments brings a dramatic impact in fields of biology, materials science, tribology, surface physics, and medical diagnosis [3,4]. Apart from their impact on science, these advances are fueling new technologies. For example, the ability to manipulate and sense the topography of material at the nanoscale has resulted in new technologies for high-density data storage [5]. Similarly, the ability to modify material biologically is leading to bio-molecular assays that can be used for drug discovery [6]. However, still many hurdles have to be overcome before the goal of *practical, reliable and routine* control and manipulation of matter at atomic scale is realized.

Precision in positioning plays an important role in performance of AFM since typically positioning systems have relatively lower open-loop bandwidth (typically an order or more smaller) than cantilevers and thus accuracy in positioning decides the quality of images in AFM. Generally, AFM scanner uses piezoelectric actuators since they provide high precision (sub-nanometer scale), have fast response, have no backlash and no wear, require little maintenance, provide relatively large forces, are invulnerable to magnetic fields, low temperature and low pressure. However, they suffer from some nonlinear effects such as hysteresis, and creep [7]. Many efforts that include feedforward designs and feedback designs have been reported to diminish these nonlinear effects and to improve the performance [8–12]. Feedforward designs are very sensitive to accuracy in models and therefore are not very robust to modeling uncertainties, and the current research in this direction focuses on obtaining robust mechanisms. Feedback designs do provide robustness to modeling uncertainties, in addition to improved performance, but are still limited by fundamental limitations that bind them.

More recently, two-degree-of-freedom (2DOF) designs that combine the feedforward and feedback strategies have been reported [8, 13–15]. In [14], 2DOF design schemes are discussed where optimal inversion control (as well as iterative learning schemes [16]) are used along with the feedback control to get improvements on the feedback-only design. In [15], a polynomial-based feedback controller is designed to account for pole-location uncertainty along with inversion based-feedforward controller which provides improved tracking for

*Address all correspondence to this author. This work was supported by NSF Grant Nos. ECS 0449310 CAR and CMMI 08-00863.

raster-scan applications. We are developing an optimal-control based framework for a systematic study of the 2DOF controllers with respect to nanopositioning, which aims at simultaneously achieving multi performance objectives in an optimal-control setting [17]. In this paper, we extend on this framework where we present new designs, review, compare, and analyze the optimal-control methods for designing 2DOF feedback laws for nanopositioning. More specifically, we study fundamental limitations on the space of achievable performance specifications in the schemes presented and study the extent of improvements of the 2DOF control designs over the feedback-only designs by comparing the roles of feedforward and feedback components of 2DOF design. Accordingly, we present and compare (1) an optimal prefilter model matching design for a system with an existing feedback controller, (2) a 2DOF optimal robust model matching design, and simultaneous feedforward and feedback control design in (3) an optimal $\mathcal{H}_\infty$ stacked sensitivity framework, and (4) a linear-matrix-inequalities (LMI)-based optimal control framework. We demonstrate the efficacy of each design through experiments on a nanopositioning scanner. Experimental results indicate substantial improvements (over 200%-300% in bandwidth) when compared to optimal feedback-only controllers.

2 2DOF framework and performance objectives

Figure 1 represents a closed-loop nanopositioning system with a 2DOF controller. In this figure, G is the transfer function of the *scanner* which comprises the positioning flexure stage, the actuating and the sensing components of the positioning system. Here y, u, r, d, n, and y_m represent the flexure stage displacement, the input given to the actuator, the reference to be tracked, the *mechanical noise*- the effects of unmodeled dynamics, the sensor noise, the noisy measurement, respectively; and the transfer functions K_{ff} and K_{fb} represent the feedforward and feedback control transfer functions, respectively. The main objective for the design of the controllers K_{ff} and K_{fb} is to make the *tracking error* small (how small is determined by the resolution requirement) over as large a bandwidth as possible while accounting for modeling uncertainties.

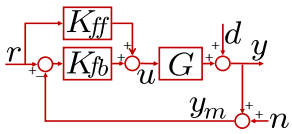

Figure 1. 2DOF control architecture: The feedforward-feedback scheme where the actuation signal $u = K_{ff}r + K_{fb}(r - y_m)$.

In 2DOF scheme, the robustness to modeling uncertainties as well as resolution of the device are determined only by the feedback part of the controller, that is the transfer function from d to y that characterizes robustness to modeling uncertainties is determined by the sensitivity function $S = (1 + GK_{fb})^{-1}$, and the transfer function from n to y that characterizes resolution is determined by the complementary sensitivity function $T = (1 + GK_{fb})^{-1}GK_{fb}$. The main difference and advantage in 2DOF control design compared to the feedback-only design stems from the fact that the transfer functions from r to y and from n to y are different and can be designed independently. This difference gives greater independence in designing for better trade-offs between different performance objectives. In this setting, the relevant closed-loop signals are given by

$$y = T_{yr}r - Tn + Sd,\ e = S_{er}r + Tn - Sd, \qquad (1)$$
$$u = S(K_{ff} + K_{fb})r - SK_{fb}n - SK_{fb}d,$$

where T_{yr} and S_{er} denote the transfer function from r to y and from r to e, respectively, that is $S_{er} = S(1 - GK_{ff})$, $T_{yr} = SG(K_{ff} + K_{fb})$. The control objectives translate to small roll-off frequency as well as high roll-off rates for T to have good resolution, long range of frequencies for which S_{er} is small to achieve large bandwidth, and low (near 1) values of the peak in the magnitude plot of S for robustness to modeling uncertainties.

3 2DOF control designs in optimal-control framework

The algebraic limitations (such as finite-waterbed effect from bode-integral law) and practical limitations (such as actuator-saturation limits and sampling-rate limits) on the control design severely restrict the space of achievable performance specifications [17–19]. The model-free based designs (such as proportional-integral-derivative (PID) designs) that are typically used in nanopositioning industry as well as designs based on loop-shaping of the open-loop transfer functions further restrict the achievable space due to their inherent structural limitations. These techniques are inadequate to achieve *simultaneously* the multiple objectives of resolution, bandwidth, and robustness under the design challenges and fundamental limitations. The robust optimal-control theory provides an apt framework for control design of nanopositioning systems. In this framework, it is possible to determine if a set of design specifications are feasible, and when feasible the control law K is obtained by posing and solving an optimization problem. The main advantage of using this optimization framework is that it incorporates performance objectives directly into its cost function. This eliminates the tedious task of tuning gains (in trial-and-hit manner) as in the PID designs, where even the exhaustively tuned gains may fail to yield acceptable performance. These optimization problems are of the form

$$\min_K \|\Phi(K)\|, \qquad (2)$$

where Φ is a matrix transfer function whose elements are in terms of closed-loop transfer functions in (1) and $\|(\cdot)\|$ represents a metric on transfer functions. The design specifications are interpreted in terms of closed-loop signals z (such as tracking error e in (1)) and then Φ is set as the transfer function from external variables w (such as reference signal r and noise n) to signals z, that is, $z = \Phi w$. Demonstration of this framework and discussion of its advantages are presented through different designs and corresponding experimental results in the following sections.

All demonstrations of the control designs in this section are preformed on a two-dimensional flexure scanner of MFP-

3D from Asylum Research Inc., Santa Barbara, CA. Physical modeling is difficult due to its complicated structural design and poorly understood piezoactuation phenomena. Therefore, identification techniques were used to derive linear models about an operating point. Weighted iterative least square fitting was performed over $0-1$ kHz and the reduction through balanced realization [20] resulted in the following 7th order model, which roles the nominal plant for the control design, $G_{xx}(s) = \frac{-1122.3157(s-1.152\times10^4)(s+543)(s^2+587.2s+8.628\times10^6)(s^2+226.5s+1.407\times10^7)}{(s+390.3)(s^2+470.9s+8.352\times10^6)(s^2+689.4s+1.315\times10^7)(s^2+4950s+2.44\times10^7)}$.

(I) Optimal prefilter model matching design

In some positioning systems, there is a pre-designed feedback component K_{fb} which cannot be replaced or changed (for instance, some commercial scanners come with feedback components designed to accomplish specific tasks such as raster scanning). However, typically there is no such restriction on the feedforward control design since it can be easily implemented as a prefilter on the reference signal. In the design presented here, the feedforward component K_{pre} is so chosen that the closed-loop positioning system mimics a *target* transfer function T_{ref} (see Figure 2 (a)). This target transfer function T_{ref} is chosen so that it satisfies desired performance objectives. An advantage of using such model matching schemes is that desired transient characteristics (such as settling times and overshoots) can be incorporated by choosing appropriate model T_{ref}, and since the closed-loop device is designed to mimic the model, it inherits the transient characteristics too. After noting that the closed-loop device transfer function from r to y is given by TK_{pre}, the feedforward component K_{pre} is chosen by solving an optimization problem such that the $\mathcal{H}_\infty$-norm of the mismatch transfer function $\Phi = T_{ref} - TK_{pre}$ is minimized. Small values of $\|\Phi\|_\infty$ guarantees small values for mismatch error signal given by

$$e = T_{ref}r - y = (T_{ref} - TK_{pre})r =: z. \tag{3}$$

To ensure practical implementation, it is assumed that T_{ref} and T are stable, proper transfer functions.

This optimization problem is trivial if T is a minimum phase transfer function, that is if it has only stable zeros. In this case T^{-1} is stable and the solution K_{pre} can be easily obtained as $T^{-1}T_{ref}$. However, typical nanopositioning systems are flexure-based with non-collocated actuators and sensors, which typically manifest as non-minimum phase zeros of T. In this case, we derived the optimal solution by applying Nevanlinna-Pick theory [21].

The model-matching problem is equivalent to finding minimum γ such that $\|T_{ref} - TK_{pre}\|_\infty \leq \gamma$, where the minimum $\gamma = \gamma_{opt}$ is achieved for some stable K_{pre}. If we define $E_\gamma = \frac{1}{\gamma}(T_{ref} - TK_{pre})$ for $\gamma > 0$, then this problem can be restated as finding a stable K_{pre} which requires $\|E_\gamma\|_\infty \leq 1$. Note that, for stable K_{pre}, E_γ satisfies the interpolating conditions $E_\gamma(z_i) = \frac{1}{\gamma}T_{ref}(z_i)$ for every non-minimum phase zero z_i of the scanner G. Therefore, we can cast this as a Nevanlinna-Pick (NP) problem - of finding a function E_γ in the space of stable, complex-rational functions such that it interpolates $\{(z_i, E_\gamma(z_i))\}_{i=1}^n$. In fact, it can be shown that γ_{opt} is equal to the square root of the largest eigenvalue of the matrix $A^{-\frac{1}{2}}BA^{-\frac{1}{2}}$ where the elements of matrix A and B are respectively [21] $a_{ij} = \frac{1}{z_i+\bar{z_j}}$, $b_{ij} = \frac{b_i\bar{b_j}}{z_i+\bar{z_j}}$.The prefilter is given by

$$K_{pre} = T^{-1}(T_{ref} - \gamma_{opt}E_\gamma). \tag{4}$$

Experimental results: For the purpose of illustration, a feedback "pre-existing controller" was designed based on $\mathcal{H}_\infty$ stacked sensitivity synthesis framework of feedback-only control design, which achieves much better bandwidth when compared to PI/PID designs [11], for the same specifications on resolution and robustness. Therefore, the improvements resulting on application of our model matching prefilter shown in this paper are even more substantial when applied to typical scanners that typically have PI/PID based feedback controllers. This feedback-only design yielded a bandwidth of 49.4 Hz, the roll-off frequency of 60.1 Hz, and $\|S\|_\infty$ of 1.15 for the closed-loop device (represented by dashed lines in Figure 2 (b,c)). The prefilter is designed to T with $T_{ref} = \frac{1}{0.0003s+1}$ by using the Nevanlinna-Pick (NP) solution. The control law from NP solution is improper and has relative order of degree -2, and therefore the weight function $W_0 = \frac{1.25}{(1\times10^{-4}s+1)^2}$ is multiplied such that it becomes proper and matches the DC output gain. Figure 2(b,c) shows that this 2DOF design yields an improvement of over 330% in bandwidth over the feedback-only design. Since the feedback component of the two designs are the same and completely determines the robustness to modeling errors (characterized by $\|S\|_\infty$) as well as the positioning resolution (the roll-off frequency ω_T of T), the resolution and the robustness remain the same for both the devices.

(II) 2DOF optimal robust model matching design

In some nanopositioning systems, the issue of robustness to modeling uncertainties is critical. The systems with predesigned feedback control have satisfactory performance (resolution and bandwidth) when experiments are conducted very carefully 'near nominal' operating conditions. However, there is rapid degradation of performance (sometimes even become unstable) when the operating conditions deviate from the nominal condition.

Here, we pose an optimal control design problem that simultaneously designs a wrap-around feedback controller for robustness as well as the feedforward controller for better bandwidth. A 2DOF control design developed in [22, 23] is adopted, which uses model matching where the transfer function of the closed-loop device is made to match a pre-specified target transfer function T_{ref}. In this design formulation, the modified scanner system is represented by $G_s = GK_s$ where G represents the scanner and K_s represents the preexisting controller or open-loop shaping weight. The corresponding 2DOF optimal control problem can be explained in terms of Figure 2(d). The optimization routine seeks $K = [K_r\ K_y]$ such that the closed-loop system guarantees 'optimal' robustness to modeling uncertainties as well as minimizes the mismatch between the the transfer function from r to

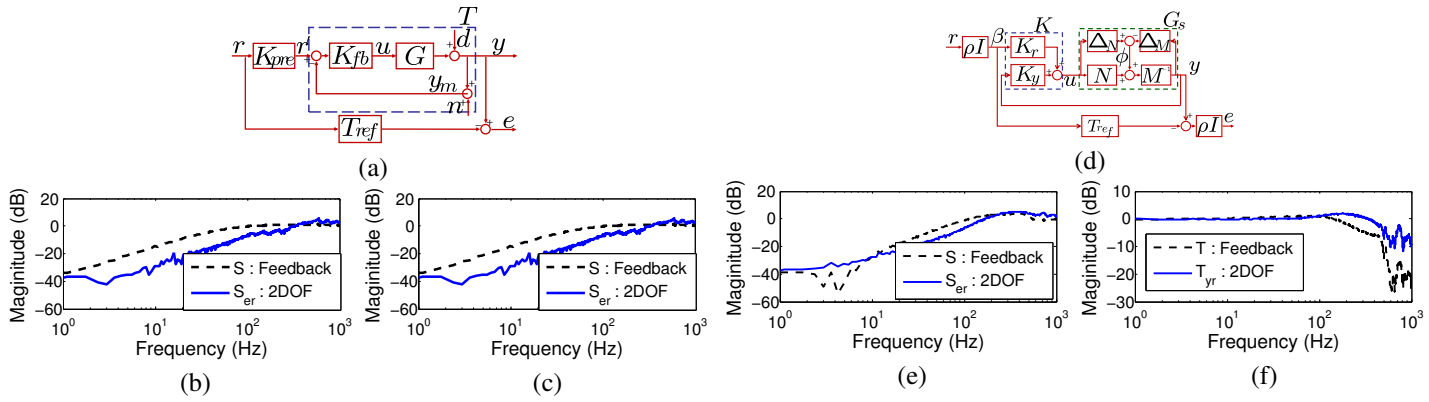

Figure 2. (a) Model matching through prefilter problem. (b,c) Comparison of experimentally obtained magnitude of $S(s)$ and $T(s)$ from $\mathcal{H}_\infty$ feedback-only control design(dashed) with $S_{er}(s)$ and $T_{yr}(s)$ from 2DOF prefilter model matching control(solid). (b) The transfer functions from reference to error i.e. S of feedback control and S_{er} of 2DOF control which represents the tracking performance (ω_{BW}=49.4Hz(feedback), =214.5Hz(2DOF)) (c) The transfer functions from reference to output i.e. T of feedback control and T_{yr} of 2DOF control. (d) Control design for model matching and robustness to modeling errors. (e,f) Comparison of experimentally obtained magnitude of $S(s)$ and $T(s)$ from PII feedback-only control design(dashed) with $S_{er}(s)$ and $T_{yr}(s)$ from 2DOF optimal robust model matching control(solid). (e) The transfer functions from reference to error i.e. S of feedback control and S_{er} of 2DOF control which represents the tracking performance (ω_{BW}=81Hz(feedback), =133Hz(2DOF)) (f) The transfer functions from reference to output i.e. $T(s)$ from feedback control and $T_{yr}(s)$ from 2DOF control.

y and a target transfer function T_{ref}. The condition for robustness is imposed by requiring the controller to guarantee stability for a set of transfer function models that are 'close' to the nominal model G_s. More specifically, the optimal control problem is cast in such a way that the resulting controller guarantees the stability of the closed-loop positioning system where the shaped scanner system is represented by *any* transfer function G_p in the set $\{G_p | G_p = (M-\Delta_M)^{-1}(N+\Delta_N), \text{where } \|[\Delta_M\ \Delta_N]\|_\infty \le \gamma^{-1}\}$, where $G_s = M^{-1}N$ is a coprime factorization [24], $[\Delta_M\ \Delta_N]$ represents the uncertain (unmodeled) dynamics, and γ specifies a bound on this uncertainty.

The controller K is obtained from minimization of the $\mathcal{H}_\infty$ norm of transfer function $\Phi(K)$ from $w = [r\ \phi]^T$ to $z = [u\ y\ e]^T$ described by

$$\begin{bmatrix} u \\ y \\ e \end{bmatrix} = \underbrace{\left[\begin{array}{c|c} \rho K_r S & K_y S M^{-1} \\ \hline \rho G_s K_r S & S M^{-1} \\ \hline \rho^2 (G_s K_r S - M_0) & \rho S M^{-1} \end{array}\right]}_{=:\Phi(K)} \begin{bmatrix} r \\ \phi \end{bmatrix}, \qquad (5)$$

where $S = (I - G_s K_y)^{-1}$. Here, the exogenous signal ϕ represents a disturbance signal that is the effects of unmodeled dynamics. Thus by making the norm on matrix transfer function small, we make the closed-loop device insensitive to the effects of unmodeled dynamics. For instance, the smaller the $\|\Phi(K)\|_\infty$ is, the smaller is effect of the disturbance ϕ on the mismatch signal e. This implies that mismatch signal has been made insensitive to the modeling errors. The signals u and y are incorporated as regulated variables in the optimization problem to account for control-saturation constraint and for noise attenuation, respectively.

Experimental results: Proportional-integral (PI) and proportional-integral-integral (PII) controllers are the most common controllers currently used in commercial scanning-probe microscopes. After an exhaustive search over the space of controller parameters to meet the performance and robustness requirement, $k_p = 0$ was chosen to get the roll-off rate of 2 for high frequency noise attenuation and $k_i = 1.1 \times 10^3$ and $k_{ii} = 6.2 \times 10^4$ were chosen to meet the bandwidth and robustness requirements (i.e. $K_{PII} = k_p + \frac{k_i}{s} + \frac{k_{ii}}{s^2}$). The 2DOF optimal robust control design was applied to G_{xx} with $K_s = K_{PII}$, $\rho = 3$, $T_{ref} = \frac{1}{0.0003s+1}$.

Figure 2(e,f) shows that the 2DOF optimal robust model matching controller achieves over 64% improvement in the tracking bandwidth. Comparison of S (not shown here) shows the improvement of robustness ($\|S\|_\infty$ = 1.52 (feedback), = 1.21 (2DOF)) which means this design process improves the bandwidth and robustness at the same time for fixed resolution which is generally impossible due to fundamental limitations in feedback-only design. This design achieves robustification and model matching simultaneously and wraps around the preexisting control. Accordingly, the closed-loop system with this design achieves better robustness to modeling errors and tracking bandwidth compared to the system with only pre-existing controller. However, if the pre-existing controller results in closed-loop device that is robust to modeling errors but has insufficient bandwidth, then this process increases the bandwidth without adversely affecting the robustness and vice versa.

(III) 2DOF stacked sensitivity synthesis

In this scheme, both the feedforward and the feedback control laws are solved simultaneously in an optimal control setting. The regulated output z was chosen as $[W_S e\ W_T y\ W_u u]'$ to reflect the performance objectives and physical constraints (see Figure

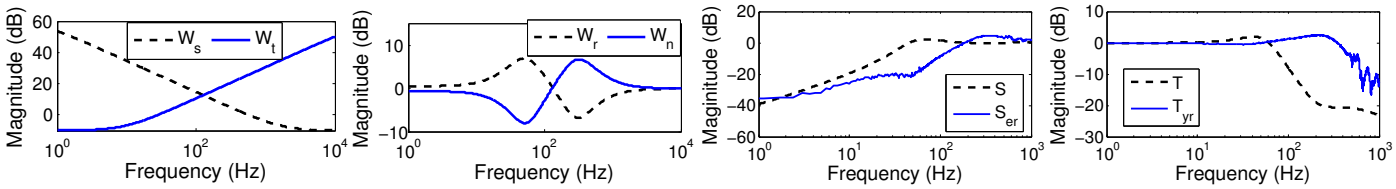

Figure 4. ((a,b) Choice of weight functions. (c) The transfer function from the reference to the error, i.e. $S_{er}(s)$, which represents the tracking performance (ω_{BW} = 148.2 Hz), and the transfer function from the disturbance to the error, i.e. $S(s)$. (d) The transfer function from the reference to the output, i.e. $T_{yr}(s)$, and the transfer function from the noise to the output, i.e. $T(s)$ (ω_T = 75.4 Hz)

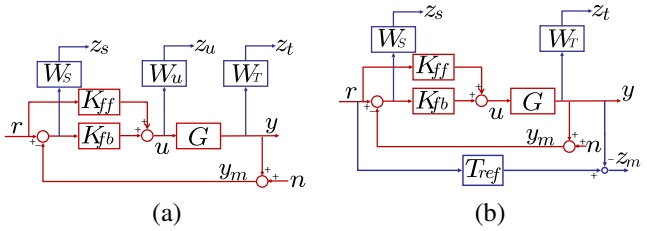

Figure 3. (a) Stacked sensitivity problem for 2DOF control design.2DOF stacked sensitivity with model matching design.

3(a)). However, 2 weight functions W_S and W_T are not enough to shape S_{er}, T_{ry}, S and T, thus the weights W_r and W_n are included to reflect their frequency content as well as obtain greater independence in specifying trade-offs to the optimization problem.

Thus Φ, the transfer function from weighted $w = [r\ n]'$ to z is given by

$$\begin{bmatrix} z_s \\ z_t \\ z_u \end{bmatrix} = \underbrace{\begin{bmatrix} W_S S_{er} W_r & -W_S S W_n \\ W_T T_{yr} W_r & -W_T T W_n \\ W_u S(K_{ff}+K_{fb}) W_r & -W_u S K_{fb} W_n \end{bmatrix}}_{=:\Phi(K)} \begin{bmatrix} r \\ n \end{bmatrix}. \quad (6)$$

Accordingly, the $\mathcal{H}_\infty$ optimal control problem $\min_K \|\Phi(K)\|_\infty$ seeks $K = [K_{ff} \quad K_{fb}]$. The minimization of z_s reflects the tracking-bandwidth requirement. If we design the *weight function* $W_S(j\omega)$ to be large in a frequency range of $[0\ \omega_{BW}]$ and ensure that z_s is small over the entire frequency range (through the above optimization problem) then the tracking-error e will be small in the frequency range $[0\ \omega_{BW}]$; that is the closed-loop positioning device has a bandwidth of ω_{BW}. Alternatively, note that the transfer function from r to z_s is $W_S S_{er} W_r$. The optimization problem along with our choice of W_S and W_r will ensure that the transfer function S_{er} is small in the frequency range $[0\ \omega_{BW}]$. Similarly, the transfer function from n to z_t is the weighted complementary sensitivity function $W_T T W_n$, whose minimization ensures better resolution as it forces low control gains at high frequencies, and the transfer function from r to z_u is $W_u S(K_{ff}+K_{fb})W_r$, which measures the control effort. Its minimization reflects in imposing the practical limitation of the control signals to be within saturation limits.

Experimental results: Four weight functions W_r, W_n, W_S, W_T are chosen to shape closed transfer functions: S_{er} with $W_S W_r$, S with $W_S W_n$, T_{yr} with $W_T W_r$, and T with $W_T W_n$. The performance objectives of high bandwidth, high resolution and robustness to modeling errors where reflected as follows. High resolution requires the roll-off frequency of ω_T to be small, that is T to be small beyond ω_T. This is imposed by designing the weight function $W_T = \frac{1000s+5.961\times10^4}{s+1.885\times10^5}$ to be large at high frequencies (ω_T specification was around 75 Hz). The range of frequencies where S is small (required for small tracking error) is restricted to small frequencies, since small T at high frequencies implies S to be near 1 at high frequencies. Thus, $W_S = \frac{0.3162s+3456}{s+3.456}$ ensures S is small at low frequencies and allows for its cross-over frequency to be small enough to make designed ω_T feasible. Figure 4(a,b) shows the choice of the weight functions that reflect these objectives. The choice of W_r and W_n is made such that at the frequency the W_T starts increasing, W_r starts increasing and W_n starts decreasing (in fact W_n is chosen as inverse of W_r). Note that at the frequency where W_S stop rolls off, W_r and W_n converge to 1. This choice of W_r and W_n ensures that S_{er} is small even when S is not small. This is done by exploiting that S is shaped by W_S while S_{er} is shaped by $W_S W_r$. The choice of weight function $W_u = 0.1$ restricted control signal values to be within saturation limits. Figure 4(c,d) show the improvement of 290% in tracking bandwidth ω_{BW} for same values of resolution and robustness if compared to feedback-only design and it is higher than the roll-off frequency ω_T. Similarly, improvement in other performance objectives (resolution and robustness) can be obtained by appropriately designed the weight functions.

(IV) 2DOF stacked sensitivity with model matching design

The disadvantage of 2DOF stacked sensitivity design in (III) is that it has high order controller which is not easy to implement practically. Thus, alternative methods are sought. In order to impose the performance objectives into optimal control setting, the configuration which is based on $\mathcal{H}_\infty$ stacked sensitivity framework and model-matching framework is considered as shown in Figure 3(b). Main idea in this setup is to shape the closed-loop transfer functions S and T with weighting functions W_S and W_T to achieve robust stability, disturbance rejection and noise attenuation and to make the close-loop response close to a target reference response $T_{ref}r$. The regulated outputs are chosen to be $z_m = T_{ref}r - y$, the deviation from target response, $z_s = W_S(r-n-y)$, the weighted tracking error with noise, and $z_t = W_T y$, the weighted system output. The closed-loop matrix transfer function from the exogenous inputs $w = [r\ n]^T$ to the

regulated outputs $z = [z_m\ z_s\ z_t]^T$ is given by

$$\begin{bmatrix} z_m \\ z_s \\ z_t \end{bmatrix} = \underbrace{\begin{bmatrix} T_{ref} - T_{yr} & T \\ W_S S_{er} & -W_S S \\ W_T T_{yr} & -W_T T \end{bmatrix}}_{=:\Phi(K)} \begin{bmatrix} r \\ n \end{bmatrix}. \quad (7)$$

The minimization of matrix $\Phi(K)$ in (7) does not correspond to the design objectives, since $\Phi(K)$ includes the other redundant terms T, $W_S S_{er}$ and $W_T T_{yr}$ which are not related to design objectives. Also, algebraic limitations of $S + T = I$ and $S_{er} + T_{yr} = I$ prevent from reaching satisfactory solution, since these constraints severely restrict the feasible space of controllers that make $\|\Phi(K)\|$ small.

In this approach, specifications are directly imposed on certain transfer functions instead of posing the problem in terms of regulated variables. More specifically, the transfer functions $T_{ref} - T_{yr}$, $W_S S$ and $W_T T$ are targeted. This is realizable by the multi-objective framework via linear matrix inequalities (LMI) optimization proposed in [25]. The cost objectives to be minimized are $T_{ref} - T_{yr}$ which is the transfer function from r to z_m and $-[W_S S\ \ W_T T]^T$ which is the transfer function from n to $[z_s\ z_t]^T$. The optimization problem is stated as

$$\min_{K \in \mathcal{K}} \rho \left\| T_{ref} - T_{yr} \right\|_{\alpha_1} + \left\| \begin{matrix} W_S S \\ W_T T \end{matrix} \right\|_{\alpha_2} \quad (8)$$

where $K = [K_{ff}\ \ K_{fb}]$, $\mathcal{K}$ is the set of stabilizing controllers and the parameter ρ reflects the user defined relative emphasis between model matching and robust performance and $\|\cdot\|_{\alpha_i, i \in \{1,2\}}$ are norms (generally 2-norm or ∞-norm) that can possibly be different from each other. The above optimization problem is adapted into the LMI framework and solved using regular algorithms for convex-optimization problems [20].

Experimental Results: The controller resulting from the design outlined above is applied to G_{xx} with $T_{ref} = \frac{1}{0.0003s+1}$, $W_S = \frac{0.5s+394.8}{s+0.3948}$ and $W_T = \frac{100s+9.475\times10^4}{s+1.184\times10^5}$ which reflect the performance objectives of high bandwidth, high resolution and robustness to modeling errors. High bandwidth requires that $|S_{er}|$ is small for wide operating frequency. It is imposed by T_{ref} function since matching $T_{yr} = 1 - S_{er}$ with T_{ref} shapes S_{er} indirectly. High resolution requires the roll-off frequency of ω_T to be small, which is reflected in W_T. The robustness requirement is reflected in W_S which enforces $\|S\|_\infty \leq 2$. The weight of $\rho = 20$ is chosen for the multi-objective minimization. The resulting controller was such that $\left\| T_{ref} - T_{yr} \right\|_\infty = 0.526$ and $\left\| [W_S S\ W_T T]^T \right\|_\infty = 2.48$.

The 2DOF control laws obtained from multi-objective synthesis were implemented. The experimental results are shown in Figure 5. The experimentally obtained $\|S_{er}\|$ is shown in (c) which determines the tracking bandwidth (ω_{BW}= 161 Hz), $\|S\|$ is shown in (a) which specifies the robustness to modeling uncertainties ($\|S\|_\infty$=1.06), and $\|T\|$ is shown in (b) which determines resolution (roll-off frequency ω_T=57.5 Hz). For comparison with *optimal* feedback-only 1DOF design, the feedback-only controller was designed by S/T stacked sensitivity optimal control synthesis such that the closed-loop function has similar $|T|$ and $|S|$ as shown in Figure 5 which means almost identical resolution and robustness to model uncertainty.

The experiment results in $\|S\|_\infty$=1.17, ω_T=63.7 Hz and ω_{BW}= 51.0 Hz. There is an improvement of 216% in bandwidth for nearly the same values of resolution and robustness when compared to the optimal feedback-only design. To demonstrate the tracking performance, triangular signals at different frequencies were given as reference signals and the corresponding outputs from 2DOF and 1DOF designs are plotted in Figure 5(e,f). Note that the 2DOF design performs better than the 1DOF design for high frequency signals. Note that both the 1DOF and 2DOF designs are solved for same specifications on resolution and robustness (for input-to-error gain 0.01% at low frequencies, roll off frequency for T of ≈ 60 Hz and $\|S\|_\infty < 1.2$).

4 Analysis and Discussion

(a) Practical elimination of hysteresis through proposed design: The main objective of the most feedforward-only designs is to compensate for mechanical noise d, especially hysteresis and creep - the nonlinear effects of piezoactuation. Since the feedback-part of the 2DOF designs in this paper are designed for high robustness to mechanical noise d, the resulting controllers practically eliminate hysteresis and creep. For instance Figure 6(a,b) demonstrates practical elimination of hysteresis and justification of the linear model for the LMI-based 2DOF design in section (IV). When actuation voltage is applied to an actuator gradually from -1.8 V to 1.8 V in the open-loop configuration, a maximum output hysteresis of about 3.06 μm (9.4%) and a maximum input hysteresis is about 0.32 V (9.0%) is observed. However, the feedback-control design effectively compensates this nonlinear effect. In Figure 6(b), a reference command is given to move the stage from origin to 14 μm and then retrace the same distance. The maximum output and input hysteresis is about 46 nm, only 0.2% of overall input and output range. However, as clearly seen from these experimental results, the closed-loop system gives desired (linear) motion for the entire range for motion of the system and it is insensitive to the error from simplification that we assumed in the open-loop model. Figure 6(c) shows the effect of creep. All the actuators were given command signals to move the stage to the origin and then keep it there. The corresponding result of the closed-loop system shows that the control design practically removes the creep effect.

(b) Breaking barriers of feedback-only design: The 2DOF design is not bound by some fundamental limitations that constrain the feedback-only designs. For instance the results in sections (I),(III),and (IV) show that in 2DOF design, the tracking bandwidth ω_{BW} of the closed-loop device can be made larger than the roll off frequency ω_T which determines the resolution. The corner frequency ω_{BW} can *never* be made larger than ω_T in feedback-only design, which suffers from a stricter trade-off between the resolution and the bandwidth. For instance, 2DOF prefilter model matching control based on $\mathcal{H}_\infty$ controller in section (I) has ω_{BW} of 214.5Hz and ω_T of 60.1Hz while original $\mathcal{H}_\infty$ controller has the bandwidth of 49.4Hz and the same roll-off frequency. This example gives a case where 2DOF design achieves

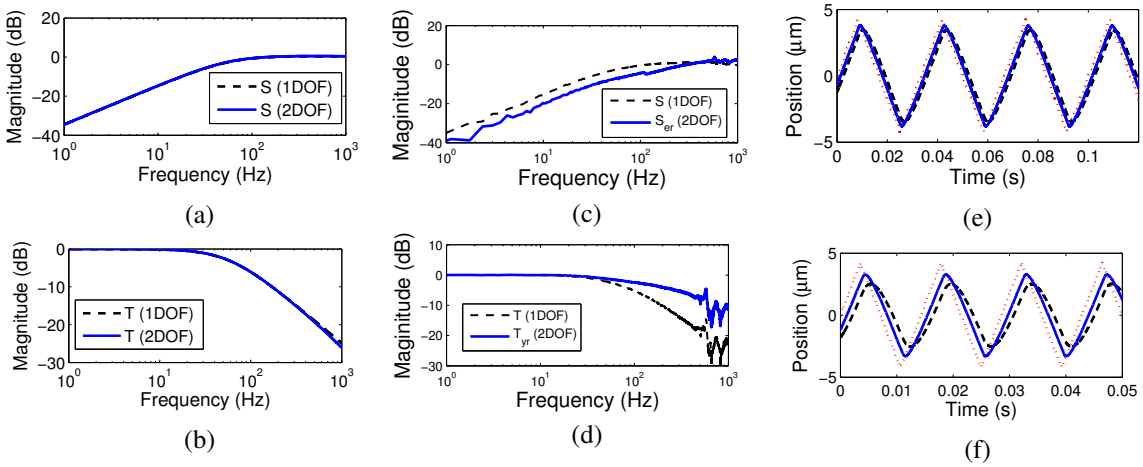

Figure 5. Comparison of 1DOF(feedback-only) $\mathcal{H}_\infty$ stacked synthesis and 2DOF multi-objective synthesis control design. (a),(b) $|S|$ and $|T|$ from 1DOF control design(dashed) with $|S|$ and $|T|$ from 2DOF control design(solid). (c),(d) $|S|$ and $|T|$ from 1DOF control design(dashed) with $|S_{er}|$ and $|T_{yr}|$ from 2DOF control design(solid) obtained from experiment. The 2DOF multi-objective synthesis control achieves about 216% improvement in the tracking bandwidth. (e,f) Triangular reference signals(dotted) with frequencies 30 Hz and 70 Hz are given. The tracking performance of 2DOF design(solid) is better than the 1DOF design(dashed), especially at high frequencies.

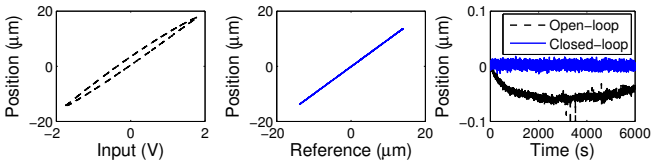

Figure 6. Hysteresis in open-loop configuration (a) and closed-loop configuration (b). (c) Creep in open-loop and closed-loop configurations. The hysteresis and creep are practically eliminated by 2DOF design.

specifications that are *impossible* to attain with feedback-only design. Similarly, the comparison of 2DOF design in section (IV) with an optimal 1DOF design shows improvement by 216% in bandwidth for the same resolution and bandwidth. Note that the 1DOF design is optimal in the sense that any change in specification for better resolution and/or robustness (in the 1DOF $\mathcal{H}_\infty$ optimal control formulation) will result in reduction of the resulting bandwidth.

(c) Relative roles of feedforward and feedback: Noting that $S_{er} = S(1 - GK_{ff})$, and S cannot be made small over the entire bandwidth range (in order to allow for noise attenuation), the feedforward control is 'active' in making S_{er} small beyond the frequency where $|S|$ is not small (say greater than $1/\sqrt{2}$). Also since $S = (1 + GK_{fb})^{-1}$ is completely determined by K_{fb}, the feedback component is dominant in frequencies where S is small. Therefore, the main contribution of feedforward component is in the frequency range where S is no longer small. However this frequency range is limited. Typically nanopositioning systems have very low gains beyond their flexure resonance frequencies. Therefore, very high control inputs are needed to make the positioning systems practical beyond their flexure resonances. The saturation limits on control signals form the main constraints on attaining bandwidths beyond flexure resonances. Thus, the feedforward components provide performance *enhancements* over feedback-only designs in the frequency range from corner frequency of S to the flexure resonance frequency. This perspective is further justified from the fact that the 2DOF stacked sensitivity optimal control designs, where the optimization problem does not discriminate between feedforward and feedback components with respect to performance objectives, exhibit this separation of their roles.

(d) Flexibility of design objective-Advantages from using LMIs: Besides possessing the advantages of 2DOF designs, one of the principal advantages of the LMI-based approach is that it allows *simultaneous* incorporation of different metrics of performance constraints such as $\mathcal{H}_\infty$, $\mathcal{H}_2$ as well as design requirements such as specifications on passivity, asymptotic tracking and pole locations [25, 26]. This generality of approach, specially incorporation of mixed norm optimization problem, proves very useful in the context of nanopositioning. The measure on robustness is well characterized by infinity norm, but the natural metrics on resolution and bandwidth can vary depending on the applications and specific requirements. For instance, the metric on model mismatch can be given in terms of $\mathcal{H}_\infty$ norm as we have considered in this paper or $\mathcal{H}_2$ norm depending on whether we are interested in the 'worst-case' or the average performance. Thus, various specifications impose different optimization problems, say in the form $\min_{K\in\mathcal{K}} \rho\|T_{ref} - T_{yr}\|_\alpha + \|T\|_\beta$ subject to $\|W_S S\|_\gamma < 1$, where α, β, and γ can be two or ∞ norms. This approach also allows for interchanging cost and constraints in an optimization problem. For instance, one can solve a problem where the cost function is maximization of robustness for given specifications of model mismatch and noise attenuation, That is, one can solve for

problems of the form $\min_{K\in\mathcal{K}} \|S\|_\infty$ subject to $\|T_{ref} - T_{yr}\|_\infty < m_1$ and $\|T\|_\infty < m_2$. Thus, this approach makes possible addressing a variety of nanopositioning applications with diverse objectives.

(e) Control-design extensions: The 2DOF designs presented here can be easily extended to achieve a larger class of design specifications than presented in this paper with trivial or no modifications to the designs presented here. For instance, we have not exploited the frequency content of the reference signals into our design. This can be easily incorporated by writing the reference signal as $r = H(j\omega)r'$, where r' is arbitrary signal (as used in our analysis) and the transfer function $H(j\omega)$ reflects the frequency content of the signal. Alternatively we can incorporate the frequency content of the reference signal through the model transfer functions T_{ref} or through weight transfer functions.

REFERENCES

[1] Binnig, G., Rohrer, H., Gerber, C., and Weibel, E., 1982. "Tunnelling through a controllable vacuum gap". *Applied Physics Letters,* **40(2)**, pp. 178–180.

[2] Binnig, G., Quate, C. F., and Gerber, C., 1986. "Atomic force microscope". *Physical Review Letters,* **56**(9), March, pp. 930–933.

[3] Bhushan, B., 1999. *Handbook of Micro/Nano Tribology*, 2nd ed. CRC Press.

[4] Meyer, E., Hug, H. J., and Benneewitz, R., 2004. *Scanning Probe Microscopy: The Lab on a Tip*. Springer, Heidelberg.

[5] Sebastian, A., Pantazi, A., Cherubini, G., Eleftheriou, E., Lantz, M. A., and Pozidis, H., 2005. "Nanopositioning for probe storage". In Proceedings of the American Control Conference, Portland, Oregon, pp. 4181– 4186.

[6] Xu, J., Lynch, M., Huff, J. L., Mosher, C., Vengasandra, S., Ding, G., and Henderson, E., 2004. "Microfabricated quill-type surface patterning tools for the creation of biological micro/nano arrays". *IEEE Transactions on Nanotechnology,* **6**(2), pp. 1387–2176.

[7] Croft, D., Shedd, G., and Devasia, S., 2000. "Creep, Hysteresis and Vibration compensation for Piezoactuators: Atomic Force Microscopy Application". In Proceedings of the American Control Conference, Chicago, Illinois, pp. 2123–2128.

[8] Leang, K., and Devasia, S., 2002. "Hysteresis, creep and vibration compensation for piezoactuators: feedback and feedforward control". In Proceedings of 2nd IFAC Conference on Mechatronic Systems, pp. 283–289.

[9] Daniele, A., Salapaka, S. Salapaka, M. V., and Dahleh, M., 1999. "Piezoelectric scanners for atomic force microscopes: design of lateral sensors, identification and control". In Proceedings of the American Control Conference, San Diego, California, pp. 253–257.

[10] Schitter, G., Menold, P., Knapp, H. F., Allgower, F., and Stemmer, A., 2001. "High performance feedback for fast scanning atomic force microscopes". *Review of Scientific Instruments,* **72**(8), August, pp. 3320–3327.

[11] Salapaka, S., Sebastian, A., Cleveland, J. P., and Salapaka, M. V., 2002. "High bandwidth nano-positioner: A robust control approach". *Review of Scientific Instruments,* **73**(9), pp. 3232–3241.

[12] Sebastian, A., and Salapaka, S., 2005. "Design methodologies for robust nano-positioning". *IEEE Transactions on Control Systems Technology,* **13**(6), pp. 868–876.

[13] Schitter, G., Allgower, F., and Stemmer, A., 2004. "A new control strategy for high speed atomic force microscopy". *Nanotechnology,* **15**(1), pp. 108–114.

[14] Zou, Q., and Devasia, S., 2004. "Preview-based optimal inversion for output tracking: application to scanning tunneling microscopy". *IEEE Transactions on Control Systems Technology,* **12**(3), pp. 375–386.

[15] Aphale, S. S., Devasia, S., and Moheimani, S. O. R., 2008. "High-bandwidth control of a piezoelectric nanopositioning stage in the presence of plant uncertainties". *Nanotechnology,* **19**(12), Mar., pp. 125503–+.

[16] Helfrich, B. E., Lee, C., Bristow, D. A., Xiaohui, X., Dong, J., Alleyne, A. G., and Salapaka, S., 2008. "Combined $\mathcal{H}_\infty$-feedback and iterative learning control design with application to nanopositioning systems". In Proceedings of American Control Conference, Seattle, WA, pp. 3893– 3900.

[17] Lee, C., and Salapaka, S. M., 2009. "Robust broadband nanopositioning: fundamental trade-offs, analysis, and design in a two-degree-of-freedom control framework". *Nanotechnology,* **20**(3), p. 035501 (16pp).

[18] Bode, H., 1945. *Network Analysis and Feedback Amplifier Design*. New York:Van Nostrand Reinhold.

[19] Freudenberg, J. S., and Looze, D. P., 1985. "Right half-plane poles and zeros and design tradeoffs in feedback systems". *IEEE Transactions on Automatic Control,* **30**(6), pp. 555–565.

[20] Dullerud, G. E., and Paganini, F., 2000. *A Course in Robust Control Theory : A Convex Approach*. Texts in Applied Mathematics, Vol. 36. Springer, Berlin, Heidelberg, New York.

[21] Doyle, J. C., Francis, B. A., and Tannenbaum, A. R., 1992. *Feedback control theory*. MacMillan, New York.

[22] Hoyle, D. J., Hyde, R. A., and Limebeer, D. J. N., 1991. "An $\mathcal{H}_\infty$ approach to two degree of freedom design". In Proceedings of the IEEE Conference on Dicision and Control, pp. 1581–1585.

[23] Limebeer, D., Kasenally, E., and Perkins, J., 1993. "On the design of robust two degree of freedom controllers". *Automatica,* **29(1)**, pp. 157–168.

[24] Vidyasagar, M., 1985. *Control System Synthesis: A Factorization Approach*. M. I. T. Press.

[25] Scherer, C., Gahinet, P., and Chilali, M., 1997. "Multiobjective output-feedback control via lmi optimization". *Automatic Control, IEEE Transactions on,* **42**(7), Jul, pp. 896–911.

[26] Boyd, S., El Ghaoui, L., Feron, E., and Balakrishnan, V., 1994. *Linear Matrix Inequalities in System and Control Theory*, Vol. 15 of *Studies in Applied Mathematics*. SIAM, Philadelphia, PA, June.